Supplementary Information

Figure 1S (a-c) is the surface SEM diagram of (1-*x*)BF-*x*BT. All samples show a uniform and dense morphology. The average grain sizes gradually decrease from 6.29μm of 0.7BF-0.3BT to 3.09μm of 0.5BF-0.5BT with increasing *x* (Figure 1S (d)). The decreasing grain size is attributed to the high melting point (1618 ℃) of BT, which raises the densification sintering temperature, and the disorder in the crystal structure that disrupts the long-range order of the crystal arrangement. Moreover, the Energy Dispersive Spectrometer (EDS) images in Figure 2S confirm the uniform distribution of elements in (1-*x*)BF-*x*BT.

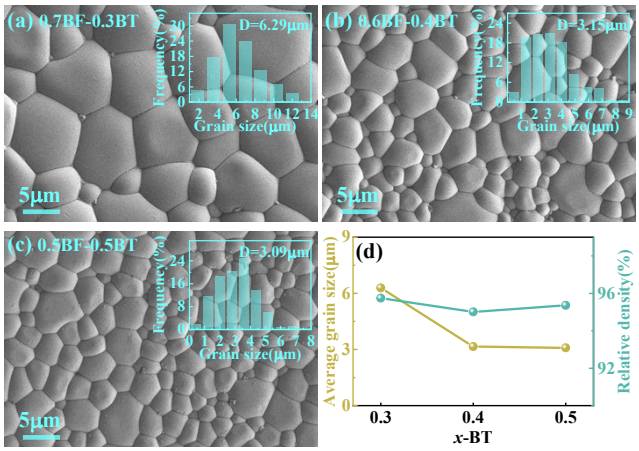

Figure 1S (a-c) Surface SEM, (d) average grain size and relative density for (1-*x*)BF-*x*BT (*x* = 0.3, 0.4, 0.5).

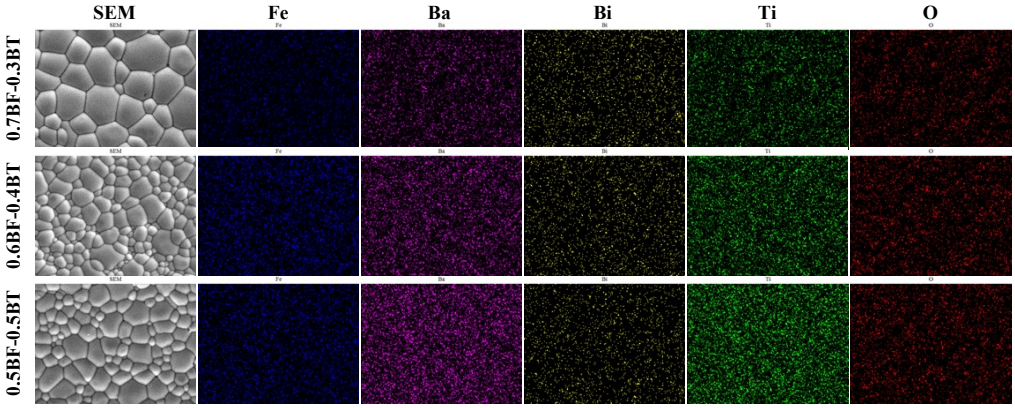

Figure 2S EDS image of (1-*x*)BF-*x*BT (*x* = 0.3, 0.4, 0.5).

Figure 3S (a) shows the impedance modulus of (1-x)BF-xBT. The modulus amplitude is only observed at $0.2 \leq x \leq 0.4$, and the amplitude is the largest at 0.7BF-0.3BT. The resonance frequency (f_r) and antiresonance frequency (f_a) can be determined from the impedance modulus. The electromechanical coupling coefficient (k_p) can be calculated by the formula:

$$\frac{1}{k_p^2} = 0.398\frac{f_r}{f_a - f_r} + 0.579$$

As BT increases, k_p reaches its maximum value at 0.7BF-0.3BT ($k_p = 0.28$). However, it is quite difficult to calculate the k_p value when $x \geq 0.5$ (Figure 3S (b)). This is consistent with variation d_{33} as a function of x.

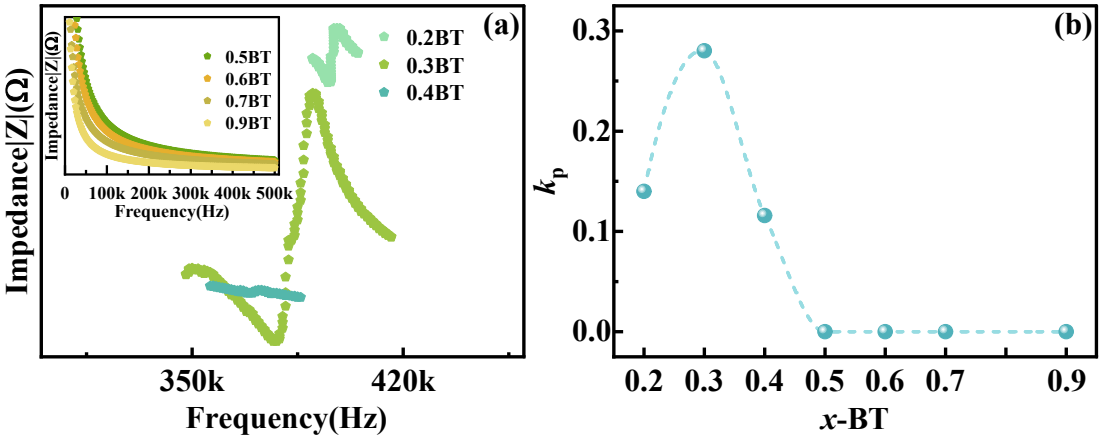

Figure 3S (a) impedance modulus and (b) k_p of (1-x)BF-xBT (x = 0.2 ~ 0.9).